

# Real-Time Implementation of a Hybrid ESC Approach for Maximising the Extracted Photovoltaic Power Under Partial Shading Conditions

Research paper

Abdelkrim Menadi<sup>1,2,\*</sup>, Fatima Zohra Boukahil<sup>2,3</sup>, Achour Betka<sup>2,3</sup>

<sup>1</sup>Abbes Laghrour University, Industrial Engineering Department, Khenchela, Algeria

<sup>2</sup>LGEB Laboratory University, Biskra, Algeria

<sup>3</sup>Mohamed Kheidher University, Electrical Engineering Department Biskra, Algeria

Received: 01 January 2024; Accepted: 06 February 2024

**Abstract:** Solar energy, an available and renewable resource, can be efficiently transformed into electrical energy through the use of photovoltaic (PV) cells. The primary emphasis lies in the significance of maximising power output for economic considerations. In terms of optimising power generation, the implementation of maximum power point tracking (MPPT) techniques is imperative. A range of approaches, such as super twisting (ST) control and modified extremum seeking control (ESC-mod), are explored for their potential in enhancing the efficiency of power-generation systems. The novelty is a combination of these methods; the modified ESC has the role of finding the optimum voltage value of the global maximum power point (MPP) during the partial shading, while the super-twisting improves the performance of the system. The efficacy of the MPPT algorithm is assessed across diverse conditions, encompassing scenarios with load variations and fluctuating irradiances (uniform and non-uniform). The experimental setup involves essential components such as a PV generator, a boost converter and a resistive load. This comprehensive testing aims to evaluate the algorithm's performance under varying circumstances, providing insights into its adaptability and effectiveness across different operational conditions. The system is modelled, simulated using Matlab–Simulink and implemented using a dSPACE 1104 card. Simulation results indicate that ST control is faster in reaching the permanent regime, but ESC-mod provides smoother performance in the permanent regime. The integration of both ST control and ESC-mod methods proves advantageous by diminishing the response time in the seeking process while concurrently ensuring a consistent and smooth operation in the permanent regime. This combined approach has undergone practical implementation and testing across diverse conditions, encompassing both optimal, healthy states and shaded environments. The results affirm the method's ability to deliver efficient and stable performance across a spectrum of operating conditions.

**Keywords:** PV panel • MPPT • modified ESC • ST-ESC modified • Global MPP

## Nomenclature

$\sigma$ : sliding surface	Rsh: array shunt resistance ( $\Omega$ )
$\alpha$ : chopper duty cycle	ST: super twisting
E: actual insolation ( $W/m^2$ )	ST-ESC mod: super twisting-extremum seeking control modified
ESC mod: modified extremum seeking control	$V_{DC}$ : actual DC link voltage (V)
$I_0$ : inverse saturation current (A)	$V_{oc}$ : PV open circuit voltage (V)
$I_{pv}$ : photovoltaic array current (A)	$V_{pv}$ : photovoltaic array voltage (V)
$I_{sc}$ : photovoltaic short circuit current	$V_{th}$ : thermal voltage (V)
$R_s$ : array series resistance ( $\Omega$ )	

\* Email: [abdelkrim.menadi@univ-khenchela.dz](mailto:abdelkrim.menadi@univ-khenchela.dz)

# 1. Introduction

Enormous research has been conducted to replace fossil fuel resources with renewable energy sources (RESs) to guarantee energy supply, diversify the energy mix and achieve short- and long-term sustainable development goals. According to the International Energy Agency (IEA), the worldwide capacity installation of RES is predicted to increase from 2,516 GW in 2018, to 6,369 GW in 2030 (Haddad et al., 2021). Algeria has taken the lead in promoting green energy by launching an ambitious plan to utilise renewable energy and improve energy efficiency. The plan aims to achieve a renewable energy generating capacity of 22,000 megawatts by 2030, including 12,000 MW for local end users and 10,000 MW for exports (Ahmad et al., 2019).

Photovoltaic (PV) systems are important renewable energy resources due to their free and clean nature. However, they have not become fully attractive as an alternative option for electricity users. Since the power generated by solar arrays depends on factors such as insolation, temperature and array voltage (Hyder et al., 2018), it is necessary to control the operating points in order to extract the maximum power from the solar array.

The tracking mechanism in this system, referred to as the maximum power point tracking (MPPT) method, is essential for searching the maximum power point (MPP) as the innate function of PV varies non-linearly with irradiance, temperature and load (Ahmad et al., 2019). A DC–DC or DC–AC converter is commonly used with an algorithm that controls the MPPT; this algorithm is known as the maximum power point tracker (Lashab et al., 2017). The most well-known and commonly used MPPT algorithm in practice is the perturb and observe (P&O) algorithm, chosen for its operational simplicity (Ali et al., 2018) (Ahmed and Salam., 2015). However, this algorithm suffers from high oscillations during steady-state operation and does not converge to the true maximum power point (Youssef et al., 2018; Harrag and Messalti., 2015).

Other algorithms, such as incremental conductance (INC) and incremental resistance, use slope regulation to detect a null derivative, as reaching the maximum value of a function requires such detection (Sera et al., 2013). These algorithms introduce disturbances into the system to evaluate the derivative of power and determine the control action. However, the need to compute derivatives in these algorithms limits their performance due to the presence of noise and singularities in numerical operations, which demonstrates that these methods and P&O have equivalent performance (Lopez-Santos et al., 2018; Xu et al., 2014).

In the literature, many classical MPPT algorithms have been proposed, such as the fractional short-circuit current and fractional open-circuit voltage (Lashab et al., 2017; Subudhi and Pradhan, 2012), but these methods also do not converge to the true MPP. Several research studies have been carried out to improve the performance of these techniques (Loukriz et al., 2016; Tey and Mekhilef, 2014; Soon and Mekhilef., 2014). As a result, recently, other adaptive algorithms, such as the sliding mode control (SMC) (Menadi et al., 2015), super twisting (ST) control (Hadj Salah et al., 2023) and extremum seeking control (ESC), have been proposed (Krstić, 2000; Leyva et al., 2006). ESC and its applications have been extensively studied, including the MPPT for the PV generators (Malek et al., 2012). One popular technique in ESC is the sliding mode-based method (Her-Terng et al., 2013; Oliveira et al., 2011; Fu and Özgüner., 2011). A developed method called SM-ESC has optimised the output of dynamic systems (Her-Terng et al., 2013).

The rest of the paper is structured as follows: Section 2 presents the modelling of the PV system components (PV generator and boost converter). Section 3 discusses the application of the hybrid MPPT algorithm (modified extremum seeking control [ESC-mod] combined with ST), while Section 4 presents the assessment of this control via simulation and implementation results. Finally, Section 5 concludes the work.

The objective of this study is to provide a real-time implementation of a hybrid ESC strategy. The purpose is to maximise the solar power produced under partial shade situations. The main focus is on overcoming the obstacles related to suboptimal power production when partial shading is present. Partial shadowing of solar panels may result in non-uniform power allocation and diminished efficiency, where several local minimums are present. The main focus of this combination is to suggest alternative control techniques to overcome the drawbacks of conventional extremum laws; used in MPPT-based control, these last methods stag in local minima and do not allow tracking the global optimum point in case of shading effects. The proposed control law gathers the skills of both the modified ESC and the STC methods to fasten the convergence mode and smooth the point in steady state. The study's implementation in real-time offers a viable and efficient way to validate the present insight, and consequently allows the feasibility of this technique in large-scale systems.

## 2. System Description and Modelling

The synoptic schematic of the studied system is shown in Figure 1. It consists of a PV array and a boost DC–DC converter that feeds a variable resistive load.

### 2.1. PV array modelling

PV arrays do not behave like traditional voltage or current sources. Instead, as depicted in Figure 2, they can be represented as voltage-controlled current sources, where their I–V characteristic can be described through an implicit equation (Betka and Attali, 2010).

$$I_{PV} = I_{sc} - I_0 \left[ \exp \left( \frac{V_{PV} + R_s I_{PV}}{V_{th}} \right) - 1 \right] \tag{1}$$

Where:

$$V_{th} = \frac{V_{op} + R_s I_{op} - V_{oc}}{\log \left( 1 - \frac{I_{op}}{I_{oc}} \right)} \tag{2}$$

$$I_0 = I_{sc} - I_{op} \left[ \exp \left( \frac{V_{op} + R_s I_{op}}{V_{th}} \right) \right] \tag{3}$$

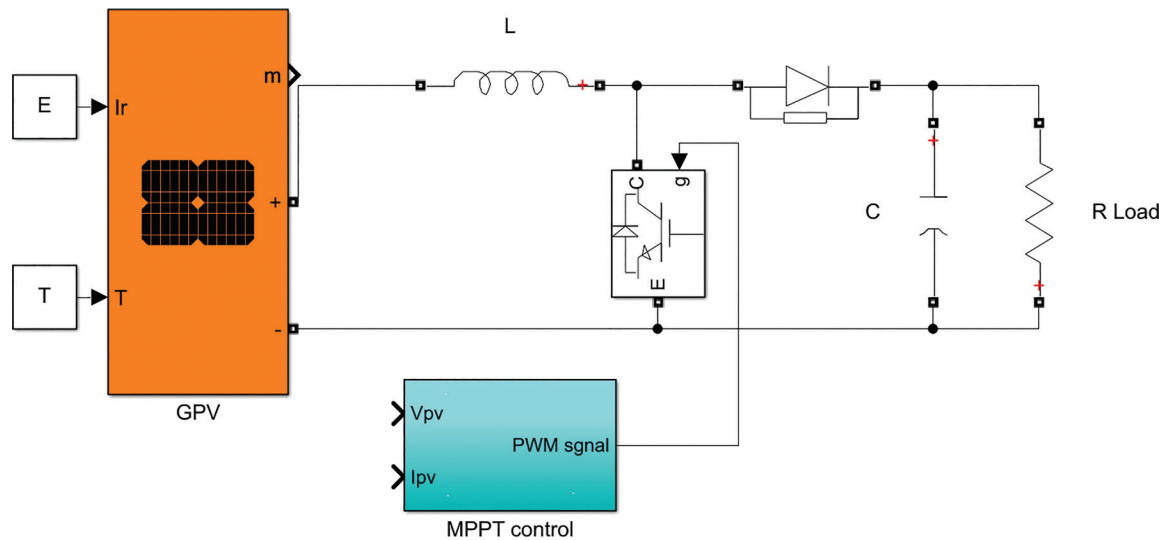


**Fig. 1.** Synoptic of the variable load connected PV system. The variables E and T denote the values of irradiance and temperature, respectively. MPPT, maximum power point tracking; PV, photovoltaic.

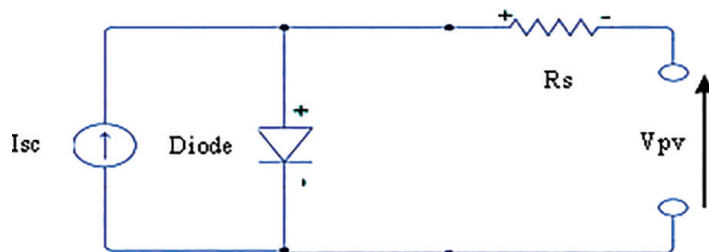


**Fig. 2.** PV panel equivalent circuit. PV, photovoltaic.

The use of Eq. (1) in variable irradiance levels can be handled via the following expressions:

$$\Delta I_{PV} = \beta \left( \frac{E}{E_r} \right) \Delta T + \left( \frac{E}{E_r} - 1 \right) I_{sc} \quad (4)$$

$$\Delta V_{PV} = \gamma \Delta T - R_s \Delta I_{PV} \quad (5)$$

$$V_{PV} = V_r + \Delta V_{PV} \quad (6)$$

$$I_{PV} = I_r + \Delta I_{PV} \quad (7)$$

## 2.2. DC/DC boost modelling

Power converters are often analysed using state-space models to assess control strategies for continuous dynamic systems. Figure 1 illustrates the derivation of the continuous dynamic model of the DC–DC boost converter. This is achieved by merging the state-space models for each switching mode with the ideal switch.

When the boost switch is off,  $S = 0$ , the following expressions are deduced for the storage elements L and C:

$$L \frac{di_L}{dt} = V_{PV} - V_{DC} \quad (8)$$

$$C \frac{dV_{DC}}{dt} = i_L - \frac{V_{DC}}{R_L} \quad (9)$$

For  $S = 1$ , these differential equations are expressed as:

$$\frac{di_L}{dt} = \frac{1}{L} V_{PV} \quad (10)$$

$$\frac{dV_{DC}}{dt} = \frac{1}{R_L C} V_{DC} \quad (11)$$

RL denotes the system's equivalent load at the DC side.

The average state-space model of the converter is obtained by combining the two equation sets (8, 9) and (10, 11) with the duty ratio  $\alpha$  (Betka and Attali, 2010):

$$\begin{bmatrix} i_L \\ V_{DC} \end{bmatrix} = \begin{bmatrix} 0 & \frac{1-\alpha}{L} \\ -\frac{1-\alpha}{C} & -\frac{1}{R_L C} \end{bmatrix} x + \begin{bmatrix} \frac{1}{L} \\ 0 \end{bmatrix} V_{PV} \quad (12)$$

## 2.3. Control approaches

The proposed MPPT control is illustrated in Figure 3 and is based on the combination of ST with the modified ESC. The general structure of the modified ESC method is derived from the conventional ESC (Boukahil et al., 2022). However, the ESC method often exhibits relatively slow transient performance.

The modified ESC algorithm has been proposed, aimed at reducing the convergence time for all MPPs. This enhancement is crucial to increase the energy yield in PV systems, particularly during abrupt changes in atmospheric conditions. The mathematical model of this modified ESC algorithm is as follows (Guay and Dochain, 2015; Tchouani Njomo et al., 2020):

ESC applied to PV systems involves a dynamic optimisation process to continually track and adjust the operating conditions for maximum power output. The classic ESC method iteratively perturbs the system's operating point and observes the resulting change in power output. Using this feedback, the control system adaptively adjusts the operating conditions, seeking to converge towards the optimal point on the power–voltage curve known as the MPP. This iterative and adaptive nature allows the PV system to effectively respond to variations in environmental factors

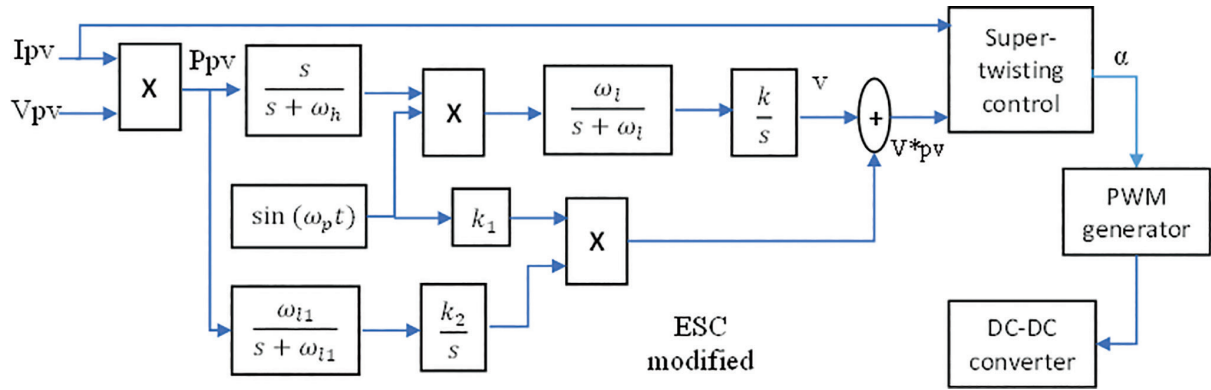


**Fig. 3.** Block diagram of the proposed ST-ESC modified control. ESC, extremum seeking control; ST, super twisting.

such as solar irradiance and temperature, ultimately enhancing the energy-harvesting efficiency by ensuring the system operates near its peak performance level.

$$\begin{cases} \frac{dv}{dt} = k\xi \\ \frac{d\xi}{dt} = \omega_l(y - \eta)\sin(\omega_p t) - \omega_l\xi \\ \frac{d\eta}{dt} = \omega_h y - \omega_h \eta \\ V_{pv}^* = f(v + \beta k_1 \sin(\omega_p t)) \end{cases} \quad (13)$$

Where:  $a = \beta k_1$ ; is the amplitude of the dither signal.

$\omega_p$ : the frequency of the dither signal.

$\omega_h$ : the cutoff frequency of the high-pass filter.

$\omega_l$ : the cutoff frequency of the first low-pass filter.

$\omega_{l1}$ : the cutoff frequency of the second low-pass filter.

$k$ : the gradient update gain.

$k_1$ : the control gain.

$V_{pv}^*$ : the voltage reference obtained by the modified ESC.

The ST control applied to a PV system involves the design of a control law to regulate the system's state variables, typically the voltage and current, to achieve a specific control objective, such as the MPPT (Kayisli, 2023). While the specific mathematical representation of the control law can vary based on the system's dynamics and desired objectives, the general form of ST control includes a sliding surface and a super-twisting algorithm.

Figure 3 depicts the proposed MPPT algorithm, which combines ST control with the modified ESC for PV systems. The approach's concept can be initiated by choosing the ST surface  $\sigma$ , which is defined as the condition for INC to capture the maximum power extraction.

$$\sigma = \frac{dI_{pv}}{dV_{pv}^*} V_{pv}^* + I_{pv} \quad (14)$$

The PV system achieves the MPP when the sliding surface equals zero ( $\sigma = 0$ ). To ensure this over the entire operating range, it is necessary for the time derivative of the quadratic Lyapunov function  $\left(V = \frac{1}{2}\sigma^2\right)$  to be negative, as shown in the following equation:

$$\dot{V} = \sigma \times \dot{\sigma} < 0 \quad (15)$$

The ST structure comprises two components:  $\alpha_{eq}$  and  $\alpha_{st}$ . The former handles the equivalent control quantity, while the latter contributes to the stabilisation aspect.

$$\alpha = \alpha_{eq} + \alpha_{st} \quad (16)$$

The value of  $\alpha_{eq}$  is obtained from the condition  $\dot{\sigma} = 0$ , which yields the conventional duty-cycle in the steady state (Rekioua et al., 2013):

$$\alpha_{eq} = 1 - \frac{V_{pv}^*}{V_{DC}} \quad (17)$$

The ST law is given by:

$$\alpha_{st} = -\lambda_1 |\sigma|^{0.5} \text{sign}(\sigma) - \int \lambda_2 \text{sign}(\sigma) dt \quad (18)$$

where the parameters of the super-twisting  $\lambda_1$  and  $\lambda_2$  are positive to fulfil system convergence.

## 2.4. Simulation and experimental results

The simulation of the control strategy used in this article is done using the MATLAB 2013b–Simulink software. The results obtained are presented in the following figures. Figure 4 presents the P–V characteristics of the PV generator, which includes two cases. The first case, called healthy case, is represented by the blue curve with an irradiance of 950 W/m<sup>2</sup>. The second case is taken under shading conditions, and it is presented by the three other curves. As shown, these plots demonstrate the influence of shading on the P–V characteristic, with each curve containing two MPPs (global point global maximum power point [GMPP] and a local one LMPP).

Figures 5 and 6, respectively, represent the GPV power curve and the static error of the previously mentioned strategies. The PV power takes only 0.006 s to achieve its optimum value using the hybrid method (super-twisting –extremum seeking modified control), while the super-twisting and modified ESC control take 0.009 s and 0.05 s, respectively, and remain stable in the steady state (STC).

Furthermore, Figure 6 confirms the efficiency of the hybrid method (a combination of super-twisting with modified ESC control). It demonstrates that the control accurately tracks the MPP, with an accuracy of around 0.027. The hybrid method outperforms the super-twisting approach.

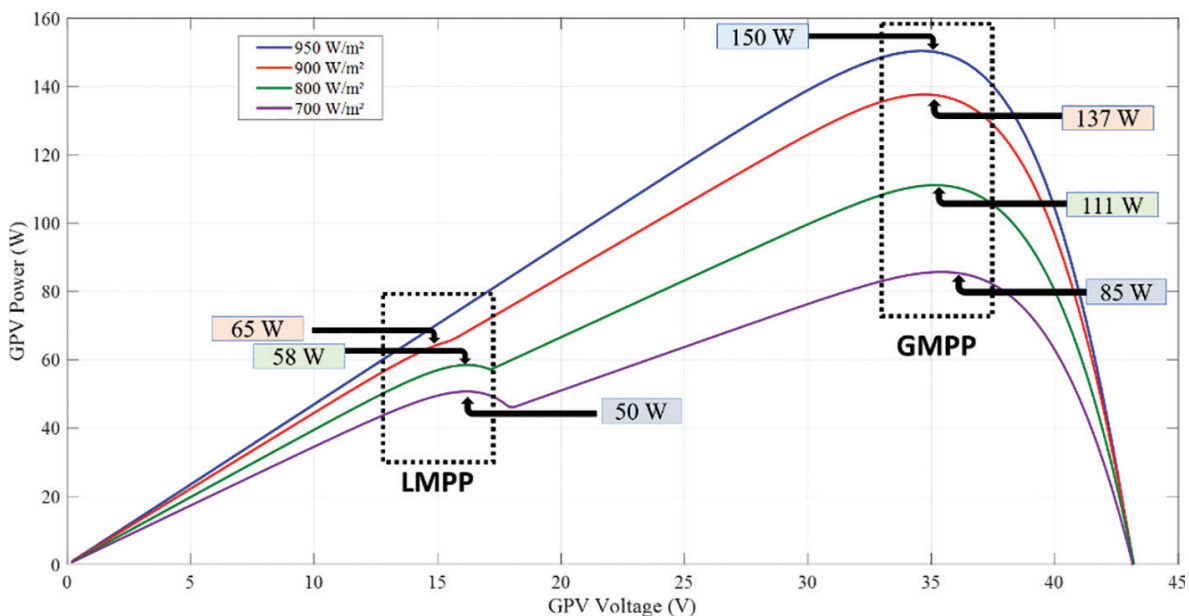
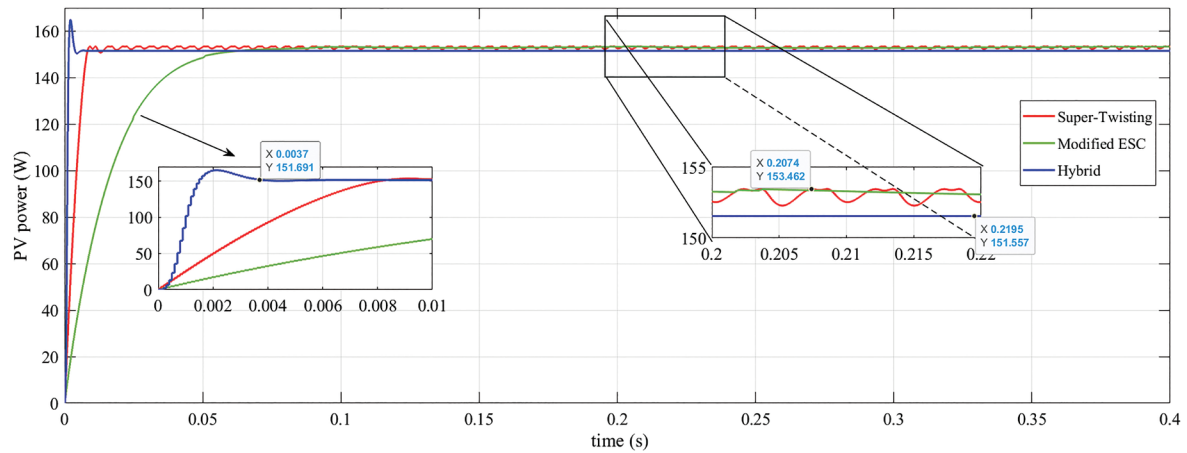
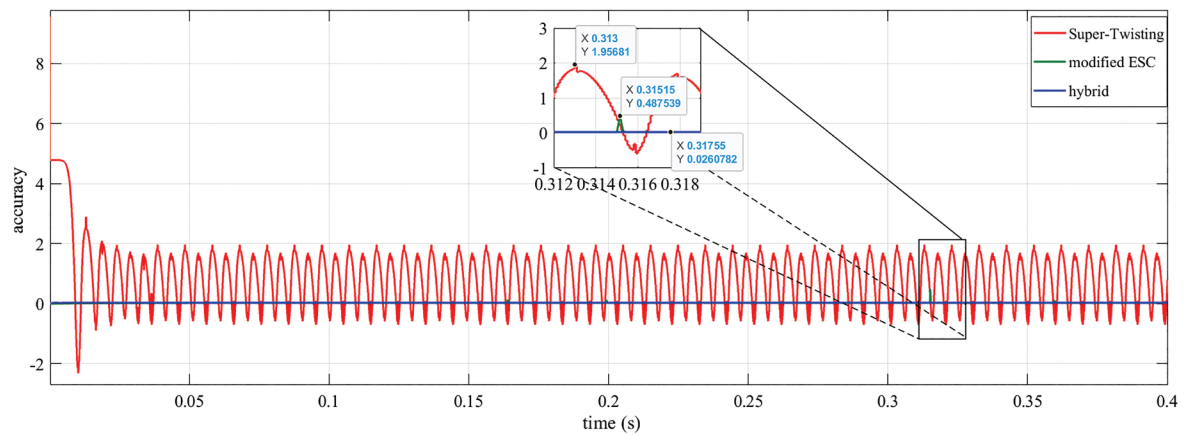


Fig. 4. Simulation of the GPV characteristics curves under shading irradiance. GMPP, global maximum power point.



**Fig. 5.** Simulation of the proposed strategies under STC. ESC, extremum seeking control; PV, photovoltaic.



**Fig. 6.** Static accuracy of the proposed MPPTs. ESC, extremum seeking control; MPPT, maximum power point tracking.

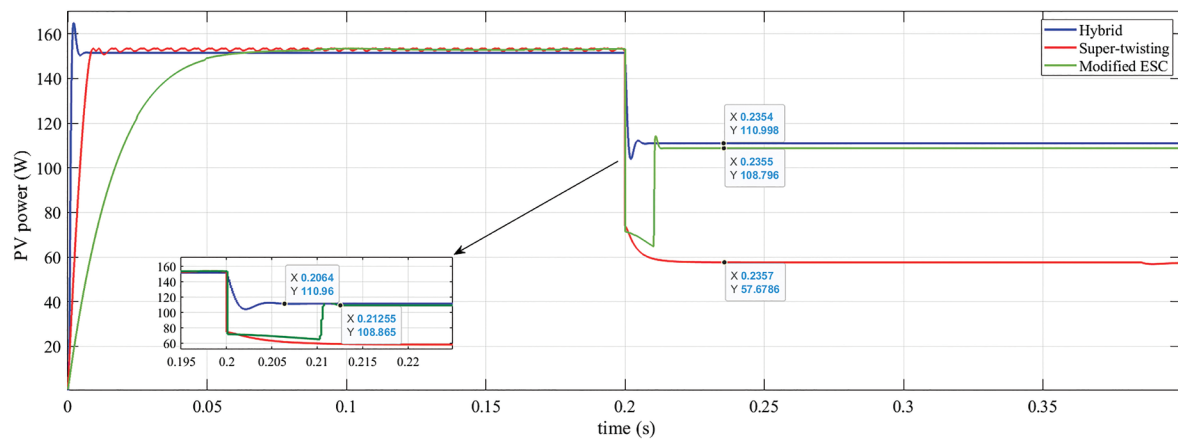


**Fig. 7.** Simulation of the algorithms for GPV power under shading irradiance. ESC, extremum seeking control; PV, photovoltaic.

Figures 7 and 8 are taken under shading conditions by applying  $800 \text{ W/m}^2$  on 50% of the PV generator surface. In Figure 7, it is evident that the hybrid method exhibits the fastest response in the transient regime and accurately follows the maximum global power during the shading condition. At 0.2 s, when shading is applied, whereas, the

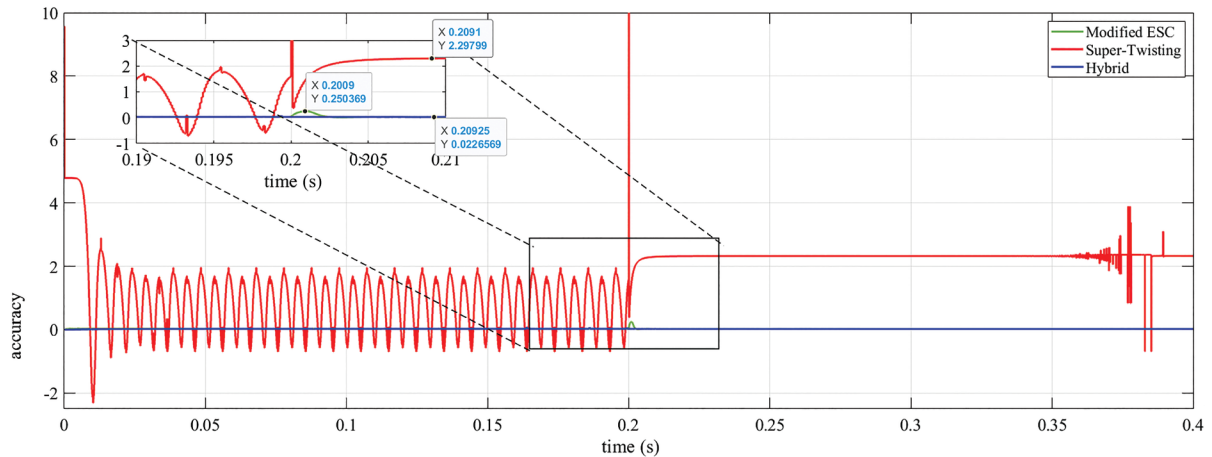


Fig. 8. Simulation of the accuracy curve under shading condition. ESC, extremum seeking control.

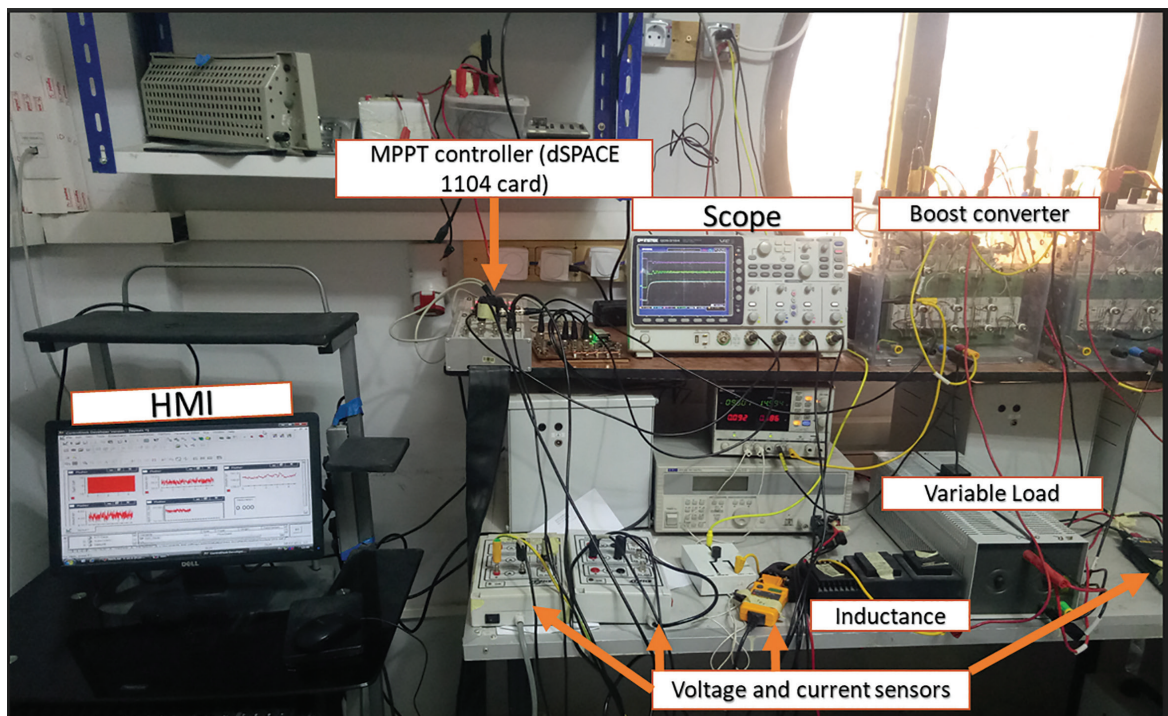


Fig. 9. Experimental test bench. MPPT, maximum power point tracking.

super-twisting goes to the local MPP (58 W), while the modified ESC and the hybrid method take 0.012 s and 0.003 s, respectively, to track the global MPP.

To implement and validate the super-twisting-ESC modified strategy developed in this paper, an experimental test bench, shown in Figure 9, was constructed in the electrical engineering laboratory of Biskra (LGEB) in Algeria. The test bench primarily comprises a 170 Wp PV generator and a boost chopper consisting of an IGBT module switch, where the parameters of the test bench and of the proposed MPPT are mentioned in the Appendix. The control algorithm is implemented using a dSPACE 1104 single card from Texas instruments with a TMS32F240 DSP, utilising the Matlab–Simulink package. An interface card connects the dSPACE card and the boost chopper, adapting the control signal levels. LA25NP and LV25P hall sensors ensure the different currents and voltages

sensing, respectively. This implementation aims to assess the robustness of the proposed MPPT regulation under both uniform and non-uniform conditions. The experimental results were obtained on a clear day with an irradiance value of  $950 \text{ W/m}^2$ .

To test the efficiency of the super-twisting-ESC modified MPPT in real-time, several tests were conducted. The first case involved uniform condition with variations in the load values, as shown in Figure 10. Additionally, more tests were performed under non-uniform condition, where shading was applied to 50% of the GPV surface with different irradiance levels, as depicted in Figures 12 and 14, respectively.

Figure 10 illustrates the GPV power and the load power behaviour. The system remained offline until the point (A) when it was turned on. The GPV's power reached its maximum point at  $150 \text{ W}$  ( $E = 950 \text{ W/m}^2$ ) in  $t_r = 0.1 \text{ s}$ . The generator's power remained stable until point (B), where a change was made in the load values of  $2 \Omega$  (from  $6.5 \Omega$  to  $8.5 \Omega$ ). The power decreased with a slight variation and quickly resumed its maximum value in  $<3 \text{ ms}$ .

The accuracy presented in Figure 11 confirms the effectiveness and reliability of the super-twisting-ESC modified MPPT in uniform conditions, including load changes. It is evident that the accuracy oscillates around  $0.05$ , even after the load variation, which proves that the controller effectively tracks the optimum power.

To ensure the effectiveness of the super-twisting-ESC modified control, more tests were applied on the system. The shading tests are presented in the following figures, wherein the system was set in real-time at the point A, and three cases of shading were applied at point C with a difference in irradiance values.

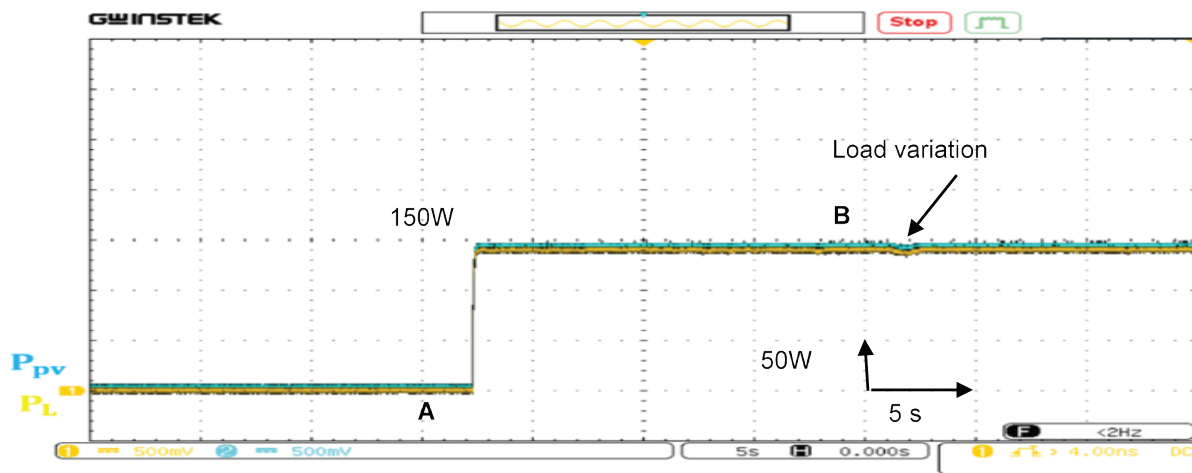


Fig. 10. Experimental curve for the GPV power in STC with load variation.

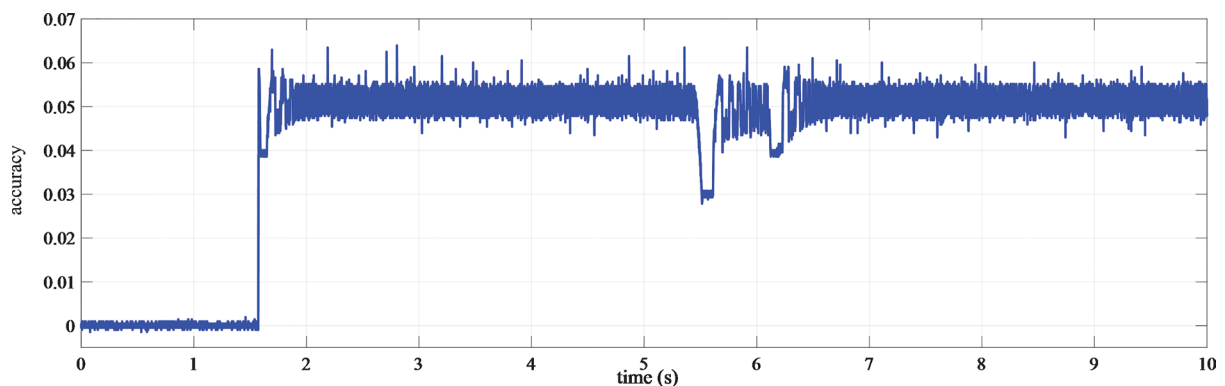


Fig. 11. Experimental curve of the accuracy.

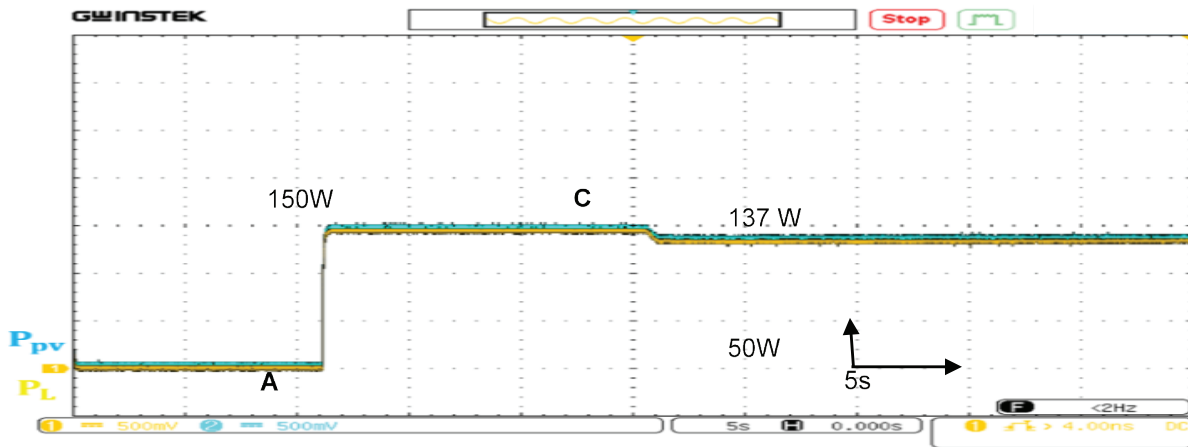


Fig. 12. Experimental curve of the GPV power under shading condition ( $900 \text{ W/m}^2$ ).

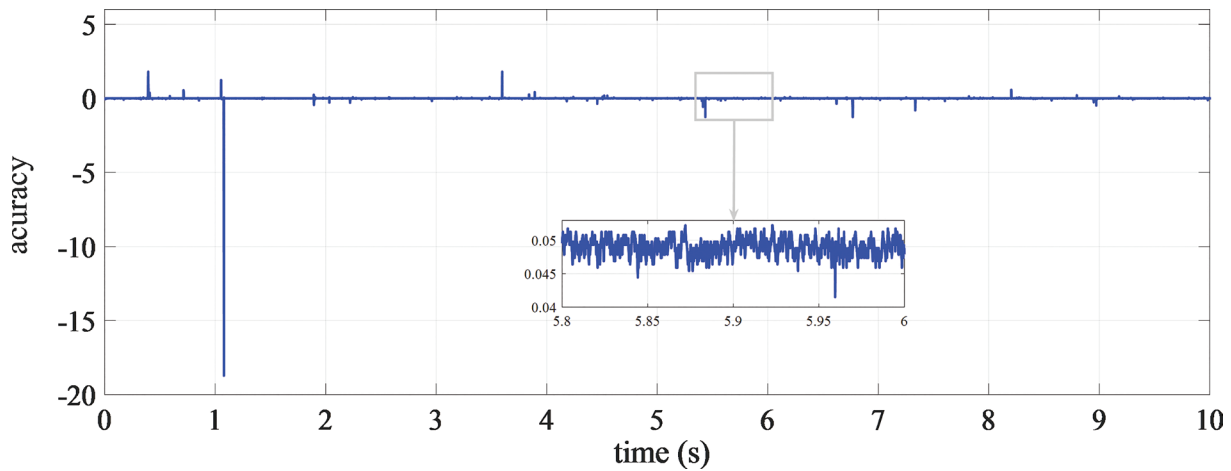


Fig. 13. Experimental accuracy of GPV system under shading ( $900 \text{ W/m}^2$ ).

### Case 1:

The first case of shading is represented in Figure 12. The generator's power reaches its maximum point value after loading the proposed controller on the dSPACE card, where the irradiance is set at  $950 \text{ W/m}^2$ . At point (C), a shadow was applied at the GPV surface, where 50% was covered with  $900 \text{ W/m}^2$  irradiance causing the GPV power to decrease to  $137 \text{ W}$ , which corresponds to the GMPP according to Figure 4. It stabilises within just  $0.4 \text{ s}$ .

Where the accuracy is the surface around the MPP,  $\sigma = \frac{dI_{pv}}{dV_{pv}^*} V_{pv}^* + I_{pv}$

Furthermore, the accuracy presented in Figure 13 demonstrates the robustness of the super-twisting-ESC modified strategy. During the first test, the accuracy remains stable around  $0.05$  in the steady state.

### Case 2:

In this case, another test is presented in Figures 14 and 15 to confirm the performances of the hybrid MPPT. This test was conducted by covering the same area of the PV generator with a different irradiance value, specifically  $800 \text{ W/m}^2$ . The steps taken to measure the PV power output were the same, and at point (C), the authors introduced shading to the GPV. As shown, the output power immediately reaches to the GMPP and stabilises within  $<0.2 \text{ s}$  in the steady state, with no losses in the load's power.

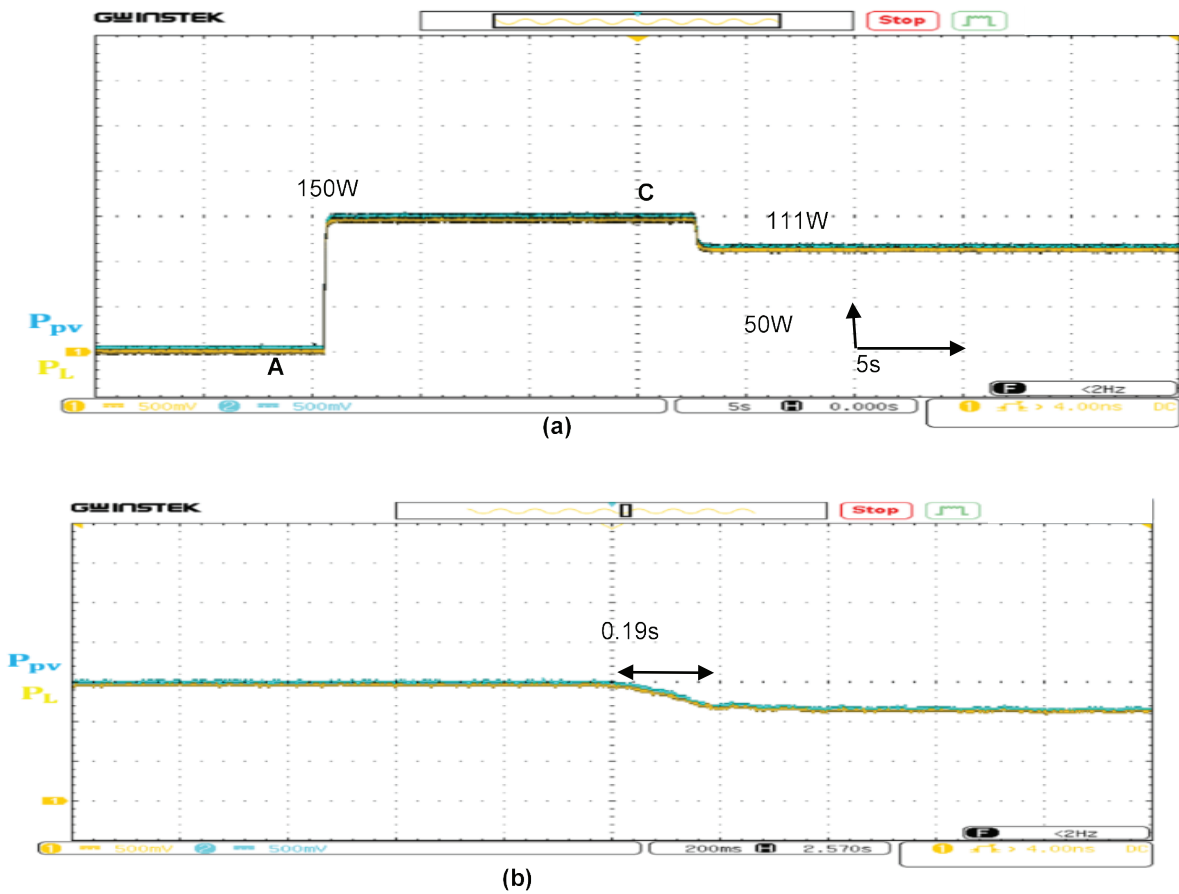


Fig. 14. (a) Experimental curve of GPV power under partial shading ( $800 \text{ W/m}^2$ ) and its zoom (b).

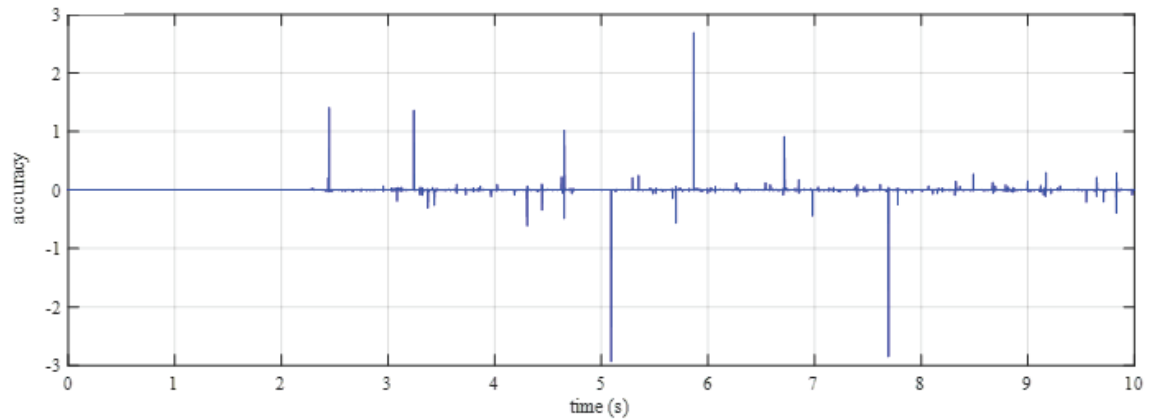


Fig. 15. Experimental accuracy curve for partial shading ( $800 \text{ W/m}^2$ ).

### 3. Conclusion

This paper discusses the tracking of the MPP in PV systems. An ESM-ST MPPT controller has been developed and verified using a simulated PV system under various atmospheric conditions in the Matlab–Simulink environment.

Subsequently, the ESM-ST controller has been implemented in real-time at the LGEB laboratory to confirm the effectiveness and robustness of the proposed controller.

The results obtained through Matlab–Simulink show a perfect extraction of the maximum PV power and excellent performance during STC and partial shading. The response time  $t_r$  is almost 0.004 s, and the static error is  $<0.05$ , comparing it to the super-twisting and ESM controllers, especially in the partial shading tests.

The experimental results confirm the effectiveness of the hybrid MPPT algorithm and show a smooth curve of the load power with no shattering during abrupt changes in atmospheric conditions.

## References

- Ahmad, R., Murtaza, A. F. and Sher, H. A. (2019). Power Tracking Techniques for Efficient Operation of Photovoltaic Array in Solar Applications—A review. *Renewable and Sustainable Energy Reviews*, 101, pp. 82–102. doi: 10.1016/j.rser.2018.10.015.
- Ahmed, J. and Salam, Z. (2015). An Improved Perturb and Observe (P&O) Maximum Power Point Tracking (MPPT) Algorithm for Higher Efficiency. *Applied Energy*, 150, pp. 97–108. doi: 10.1016/j.apenergy.2015.04.006.
- Ali, A. I., Sayed, M. A. and Mohamed, E. E. (2018). Modified Efficient Perturb and Observe Maximum Power Point Tracking Technique for Grid-Tied PV System. *International Journal of Electrical Power & Energy Systems*, 99, pp. 192–202. doi: 10.1016/j.ijepes.2017.12.029.
- Betka, A. and Attali, A. (2010). Optimization of a Photovoltaic Pumping System Based on the Optimal Control Theory. *Solar Energy*, 84(7), pp. 1273–1283. doi: 10.1016/j.solener.2010.04.004.
- Boukahil, F., Menadi, A., Abdeddaim, S. and Betka, A. (2022). Experimental Validation of Extremum Seeking and Sliding Mode-Based Control for an Autonomous PV System Under Partial Shading Conditions. *Journal of Electrical Systems*, 18(4), pp. 520–532.
- Fu, L. and Özgüner, Ü. (2011). Extremum Seeking with Sliding Mode Gradient Estimation and Asymptotic Regulation for a Class of Nonlinear Systems. *Automatica*, 47(12), pp. 2595–2603. doi: 10.1016/j.automatica.2011.09.031.
- Guay, M. and Dochain, D. (2015). A Time-Varying Extremum-Seeking Control Approach. *Automatica*, 51, pp. 356–363. doi: 10.1016/j.automatica.2014.10.078.
- Haddad, B., Díaz-Cuevas, P., Ferreira, P., Djebli, A. and Pérez, J. P. (2021). Mapping Concentrated Solar Power Site Suitability in Algeria. *Renewable Energy*, 168, pp. 838–853. doi: 10.1016/j.renene.2020.12.081.
- Hadj Salah, Z. B., Krim, S., Hajjaji, M. A., Alshammari, B. M., Alqunun, K., Alzamil, A. and Guesmi, T. (2023). A New Efficient Cuckoo Search MPPT Algorithm Based on a Super-Twisting Sliding Mode Controller for Partially Shaded Standalone Photovoltaic System. *Sustainability*, 15(12), p. 9753. doi: 10.3390/su15129753.
- Harrag, A. and Messalti, S. (2015). Variable Step Size Modified P&O MPPT Algorithm using GA-Based Hybrid Offline/Online PID Controller. *Renewable and Sustainable Energy Reviews*, 49, pp. 1247–1260. doi: 10.1016/j.rser.2015.05.003.
- Her-Terng, Y., Chih-Jer, L. and Chen-Han, W. (2013). Sliding Mode Extremum Seeking Control Scheme Based on PSO for Maximum Power Point Tracking in Photovoltaic Systems. *International Journal of Photoenergy*, 2013, pp. 1–10.
- Hyder, F., Sudhakar, K. and Mamat, R. (2018). Solar PV Tree Design: A Review. *Renewable and Sustainable Energy Reviews*, 82, pp. 1079–1096. doi: 10.1016/j.rser.2017.09.025.
- Kayisli, K. (2023). Super Twisting Sliding Mode-Type 2 Fuzzy MPPT Control of Solar PV System with Parameter Optimization Under Variable Irradiance Conditions. *Ain Shams Engineering Journal*, 14(1), p. 101950. doi: 10.1016/j.asej.2022.101950.
- Krstić, M. (2000). Performance Improvement and Limitations in Extremum Seeking Control. *Systems and Control Letters*, 39(5), pp. 313–326. doi: 10.1016/S0167-6911(99)00111-5.
- Lashab, A., Sera, D., Guerrero, J. M., Mathe, L. and Bouzid, A. (2017). Discrete Model-Predictive-Control-Based Maximum Power Point Tracking for PV Systems: Overview and Evaluation. *IEEE Transactions on Power Electronics*, 33(8), pp. 7273–7287. doi: 10.1109/TPEL.2017.2764321.
- Leyva, R., Alonso, C., Queinnec, I., Cid-Pastor, A., Lagrange, D. and Martinez-Salamero, L. (2006). MPPT of Photovoltaic Systems using Extremum-Seeking Control. *IEEE Transactions on Aerospace and Electronic Systems*, 42(1), pp. 249–258. doi: 10.1109/TAES.2006.1603420.
- Lopez-Santos, O., Garcia, G., Martinez-Salamero, L., Giral, R., Vidal-Idiarte, E., Merchan-Riveros, M. C.

- and Moreno-Guzman, Y. (2018). Analysis, Design, and Implementation of a Static Conductance-Based MPPT Method. *IEEE Transactions on Power Electronics*, 34(2), pp. 1960–1979. doi: 10.1109/TPEL.2018.2835814.
- Loukriz, A., Haddadi, M. and Messalti, S. (2016). Simulation and Experimental Design of a New Advanced Variable Step Size Incremental Conductance MPPT Algorithm for PV Systems. *ISA Transactions*, 62, pp. 30–38. doi: 10.1016/j.isatra.2015.08.006.
- Malek H., Dadras S. and Chen Y., (2012). A fractional order maximum power point tracker: Stability analysis and experiments. In: *51st IEEE Conference on Decision and Control (CDC)*, 10–13 December 2012, Maui, HI, USA: IEEE, pp. 6861–6866. doi: 10.1109/CDC.2012.6425961
- Menadi, A., Abdeddaim, S., Ghamri, A. and Betka, A. (2015). Implementation of Fuzzy-Sliding Mode Based Control of a Grid Connected Photovoltaic System. *ISA Transactions*, 58, pp. 586–594. doi: 10.1016/j.isatra.2015.06.009.
- Oliveira, T. R., Hsu, L. and Peixoto, A. J. (2011). Output-Feedback Global Tracking for Unknown Control Direction Plants with Application to Extremum-Seeking Control. *Automatica*, 47(9), pp. 2029–2038. doi: 10.1016/j.automatica.2011.05.021.
- Rekioua, D., Achour, A. and Rekioua, T. (2013). Tracking Power Photovoltaic System with Sliding Mode Control Strategy. *Energy Procedia*, 36, pp. 219–230. doi: 10.1016/j.egypro.2013.07.025.
- Sera, D., Mathe, L., Kerekes, T., Spataru, S. V. and Teodorescu, R. (2013). On the Perturb-and-Observe and Incremental Conductance MPPT Methods for PV Systems. *IEEE Journal of Photovoltaics*, 3(3), pp. 1070–1078.
- Soon, T. K. and Mekhilef, S. (2014). A Fast-Converging MPPT Technique for Photovoltaic System Under Fast-Varying Solar Irradiance and Load Resistance. *IEEE Transactions on Industrial Informatics*, 11(1), pp. 176–186. doi: 10.1109/TII.2014.2378231.
- Subudhi, B. and Pradhan, R. (2012). A Comparative Study on Maximum Power Point Tracking Techniques for Photovoltaic Power Systems. *IEEE Transactions on Sustainable Energy*, 4(1), pp. 89–98. doi: 10.1109/TSTE.2012.2202294.
- Tchouani Njomo, A. F., Kenne, G., Douanla, R. M. and Sonfack, L. L. (2020). A Modified ESC Algorithm for MPPT Applied to a Photovoltaic System Under Varying Environmental Conditions. *International Journal of Photoenergy*, 2020, pp. 1–15. doi: 10.1155/2020/1956410.
- Tey, K. S. and Mekhilef, S. (2014). Modified Incremental Conductance Algorithm for Photovoltaic System Under Partial Shading Conditions and Load Variation. *IEEE Transactions on Industrial Electronics*, 61(10), pp. 5384–5392. doi: 10.1109/TIE.2014.230492.
- Xu, W., Mu, C. and Jin, J. (2014). Novel Linear Iteration Maximum Power Point Tracking Algorithm for Photovoltaic Power Generation. *IEEE Transactions on Applied Superconductivity*, 24(5), pp. 1–6. doi: 10.1109/TASC.2014.2333534.
- Youssef, A., El Telbany, M. and Zekry, A. (2018). Reconfigurable Generic FPGA Implementation of Fuzzy Logic Controller for MPPT of PV Systems. *Renewable and Sustainable Energy Reviews*, 82, pp. 1313–1319. doi: 10.1016/j.rser.2017.09.093.

## Appendix

a) Data of the PV array at STC conditions:

$$P_{pv} = 170 \text{ W}, I_{sc} = 5.2 \text{ A}, V_{oc} = 22 \text{ V}, I_{op} = 4.77 \text{ A}, V_{op} = 17.9 \text{ V}.$$

b) Passive elements

$$L = 3 \text{ mH}, C = 1100 \text{ } \mu\text{F}, R = 10 \text{ } \Omega.$$

c) Switching frequency:  $f = 5 \text{ kHz}$ .

d) Controllers' parameters

- Super-twisting:  $\lambda_1 = 0.005, \lambda_2 = 10$ .

- Modified ESC:

$$\omega_p = 1000, \omega_h = 10, \omega_l = 100, \omega_{l1} = 100, k = 5, k_1 = 0.007.$$

- Hybrid controller:  $\lambda_1 = 0.08, \lambda_2 = 18, \omega_p = 1000, \omega_h = 15, \omega_l = 220, \omega_{l1} = 220, k = 1, k_1 = 0.03$ .